

1990

## Infinite-temperature Dynamics of the Equivalent-neighbor XYZ Model

Jian-Min Liu

*University of Rhode Island*

Gerhard Müller

*University of Rhode Island*, gmuller@uri.edu

---

Follow this and additional works at: [https://digitalcommons.uri.edu/phys\\_facpubs](https://digitalcommons.uri.edu/phys_facpubs)

---

### Citation/Publisher Attribution

Liu, J. M., & Muller, G. (1990). Infinite-temperature dynamics of the equivalent-neighbor XYZ model. *Phys. Rev. A*, 42(10), 5854-5864. doi: 10.1103/PhysRevA.42.5854  
Available at: <http://dx.doi.org/10.1103/PhysRevA.42.5854>

---

## Infinite-temperature Dynamics of the Equivalent-neighbor XYZ Model

### Terms of Use

All rights reserved under copyright.

## Infinite-temperature dynamics of the equivalent-neighbor *XYZ* model

Jian-Min Liu and Gerhard Müller

*Department of Physics, University of Rhode Island, Kingston, Rhode Island 02881-0817*

(Received 14 June 1990)

The dynamics of the classical *XYZ* model with uniform interaction is investigated by the recursion method and, in part, by exact analysis. The time evolution is anharmonic for arbitrary  $N$  (number of spins); only the cases  $N=2$  and  $\infty$  are completely integrable. For the special (uniaxially symmetric) equivalent-neighbor *XXZ* model, the nonlinearities in the equations of motion disappear in the limit  $N \rightarrow \infty$ , and the spin autocorrelation functions are determined exactly for infinite temperature: The function  $\langle S_i^z(t)S_i^z \rangle$  exhibits a Gaussian decay to a nonzero constant, and the function  $\langle S_i^x(t)S_i^x \rangle$  decays to zero, algebraically or like a Gaussian, depending on the amount of uniaxial anisotropy. For the general *XYZ* case, the  $T=\infty$  dynamical behavior includes four different universality classes, categorized according to the decay law of the spectral densities at high frequencies. That decay law governs the growth rate of the sequence of recurrents that determine the relaxation function in the continued-fraction representation. The four universality classes may serve as prototypes for a classification of the dynamics of classical and quantum many-body systems in general.

### I. INTRODUCTION

Equivalent-neighbor spin models are familiar objects in the statistical mechanics of phase transitions, where they play a role as microscopic realizations of mean-field theory.<sup>1,2</sup> Consider an array of  $N$  spins interacting via some model-specific spin-pair coupling of uniform strength  $J'$ . In order to ensure that the free energy is extensive, the coupling strength must be scaled like  $J'=J/N$ . The thermodynamic properties of the mean-field model are in general reasonably good approximations to those of lattice models with short-range interactions, provided the lattice dimensionality is sufficiently large. Discrepancies are most pronounced near critical points, but even the mean-field critical-point exponents turn out to be exact for lattice models whose dimensionality exceeds some value  $d_u$  known as the upper marginal dimensionality.<sup>3,4</sup> For the spin models discussed here, that value is  $d_u=4$ .

In forcing the equivalent-neighbor spin model to be thermodynamically well defined at all temperatures, the price to be payed is the loss of intrinsic dynamics.<sup>5</sup> For classical spins, the right-hand side of Hamilton's equation for individual spins,  $d\mathbf{S}_i/dt = -\mathbf{S}_i \times \partial H/\partial \mathbf{S}_i$ , vanishes in the limit  $N \rightarrow \infty$ . For quantum spins, the same effect results from more subtle properties. However, a nontrivial intrinsic dynamics (for  $N \rightarrow \infty$ ) can be restored, at least in the paramagnetic phase, if the spin coupling is scaled differently:  $J'=J/\sqrt{N}$ . The two scaling regimes are best understood by noting that the thermodynamic properties of the equivalent-neighbor model are governed by the mean value of the magnetization vector (which is the basis for Landau theory), whereas the dynamical properties are determined by the fluctuations about the mean value. A meaningful description of time-dependent correlation functions for equivalent-neighbor spin models based on intrinsic dynamics is then restricted to infinite temperature.<sup>6</sup>

The point of emphasis in the analysis of such correlation functions as reported in the following will primarily be the properties of their spectral densities at high frequencies and only to a lesser degree the long-time asymptotic behavior. We shall demonstrate four different types of decay for  $\omega \rightarrow \infty$  in spectral densities:  $\Phi_0(\omega) \sim \exp(-\omega^{2/\lambda})$ ,  $\lambda=0$  (compact support),  $\lambda=1$  (Gaussian decay),  $\lambda=2$  (exponential decay),  $\lambda=3$  (stretched exponential decay), which can be interpreted in terms of basic notions of classical dynamics, and for which we borrow the term "universality class" from the theory of critical phenomena. We shall point out that a classification of dynamical behavior in terms of the exponent  $\lambda$  is useful in the context of general many-body dynamics, and that the integer-valued exponents realized by the equivalent-neighbor *XYZ* model play a role similar to the "classical" critical-point exponent values in the theory of phase transitions as realized by thermodynamic equivalent-neighbor model systems.

### II. DYNAMICAL PROBLEM

The classical equivalent-neighbor *XYZ* model is specified by the Hamiltonian

$$H = -\frac{1}{2\sqrt{N}} \sum_{\substack{i,j=1 \\ i \neq j}}^N (J_x S_i^x S_j^x + J_y S_i^y S_j^y + J_z S_i^z S_j^z). \quad (2.1)$$

The equations of motion for the classical spin variables  $S_i^\alpha$  (three-component vectors of unit length) read

$$\dot{S}_i^\alpha = J_\gamma \sigma_\gamma S_i^\beta - J_\beta \sigma_\beta S_i^\gamma - \frac{1}{\sqrt{N}} (J_\gamma S_i^\gamma S_i^\beta - J_\beta S_i^\beta S_i^\gamma), \quad (2.2)$$

with  $\alpha\beta\gamma$  equal to any cyclic permutation of  $xyz$ , henceforth denoted by  $\alpha\beta\gamma = \mathcal{C}(xyz)$ . The collective-spin variable

$$\sigma = \frac{1}{\sqrt{N}} \sum_{i=1}^N \mathbf{S}_i \quad (2.3)$$

represents the vector of instantaneous magnetization fluctuation. Anticipating the result to be demonstrated in Sec. II C that the length of  $\sigma$  is of  $O(1)$ , it follows that the  $1/\sqrt{N}$  terms in (2.2) become negligible in the limit  $N \rightarrow \infty$ . The dynamical problem then reduces to a Hamiltonian system with two degrees of freedom.

### A. Collective spin motion

Summing Eq. (2.2) over all sites  $i$ , dividing by  $\sqrt{N}$ , and taking the limit  $N \rightarrow \infty$  yields the equations of motion for the collective spin:

$$\dot{\sigma}_\alpha = (J_\gamma - J_\beta)\sigma_\gamma\sigma_\beta, \quad \alpha\beta\gamma = \mathcal{C}(xyz). \quad (2.4)$$

These equations describe an effective single-spin model, an autonomous Hamiltonian system with a single degree of freedom:

$$\dot{\sigma} = -\sigma \times \frac{\partial \bar{H}}{\partial \sigma}, \quad (2.5)$$

$$\bar{H} = -\frac{1}{2}(J_x\sigma_x^2 + J_y\sigma_y^2 + J_z\sigma_z^2) = \text{const}, \quad (2.6)$$

$$\sigma = (\sigma_x^2 + \sigma_y^2 + \sigma_z^2)^{1/2} = \text{const}. \quad (2.7)$$

For the  $XXX$  model, the case with full rotational symmetry ( $J_x = J_y = J_z$ ), the collective spin is stationary,  $\sigma = \text{const}$ . In the presence of uniaxial anisotropy ( $J_z \neq J_x = J_y \equiv J$ ,  $XXZ$  model), the vector  $\sigma$  undergoes uniform rotation about the symmetry axis,

$$\begin{aligned} \sigma_x(t) &= \sigma_1 \cos(\Omega_z t + \phi_0), \\ \sigma_y(t) &= \sigma_1 \sin(\Omega_z t + \phi_0), \\ \sigma_z &= \text{const}, \end{aligned} \quad (2.8)$$

with  $\sigma_1^2 = \sigma_x^2 + \sigma_y^2$  and frequency  $\Omega_z = (J - J_z)\sigma_z$ . In the presence of biaxial anisotropy ( $XYZ$  model), the periodic motion of  $\sigma(t)$  is anharmonic. For  $0 < J_x < J_y < J_z$  the general solution reads

$$\begin{aligned} \sigma_x(t) &= a_x \text{cn}(\Omega t + \phi_0, k), \\ \sigma_y(t) &= a_y \text{sn}(\Omega t + \phi_0, k), \\ \sigma_z(t) &= a_z \text{dn}(\Omega t + \phi_0, k), \end{aligned} \quad (2.9)$$

with amplitudes, frequency, and modulus given by

$$a_x^2 = \frac{J_z\sigma^2 - 2\epsilon}{J_z - J_x}, \quad a_y^2 = \frac{J_z\sigma^2 - 2\epsilon}{J_z - J_y}, \quad a_z^2 = \frac{2\epsilon - J_x\sigma^2}{J_z - J_x}; \quad (2.10)$$

$$\Omega^2 = (J_z - J_y)(2\epsilon - J_x\sigma^2); \quad (2.11)$$

$$k^2 = \frac{J_y - J_x}{J_z - J_y} \frac{J_z\sigma^2 - 2\epsilon}{2\epsilon - J_x\sigma^2}. \quad (2.12)$$

The initial conditions are expressed in terms of the two invariants  $\sigma$  and  $\epsilon = |\bar{H}|$ , where  $J_x\sigma^2/2 < \epsilon < J_z\sigma^2/2$ , and a phase  $\phi_0$ .<sup>7,8</sup>

### B. Individual spin motion

For a given solution of  $\sigma(t)$ , the equations of motion (2.2) for individual spins are then (for  $N \rightarrow \infty$ ) linear first-order ordinary differential equations (ODE's) with time-periodic coefficients:

$$\dot{S}_i^\alpha = J_\gamma \sigma_\gamma(t) S_i^\beta - J_\beta \sigma_\beta(t) S_i^\gamma, \quad \alpha\beta\gamma = \mathcal{C}(xyz), \quad (2.13)$$

which proves that the original many-body system (2.1) is integrable in the limit  $N \rightarrow \infty$ . For finite  $N$ , integrability is, in general, destroyed by the  $1/\sqrt{N}$  corrections in Eq. (2.2).

The solution of (2.13) is especially simple for the  $XXX$  model ( $J_x = J_y = J_z \equiv J$ ).<sup>9,10</sup> Here the vector  $\sigma$  is a constant of the motion (for arbitrary  $N$ ). Each spin  $S_i$  precesses uniformly about the direction of  $\sigma$  with frequency  $\bar{\Omega} = J\sigma$ . Hence all spin configurations with zero magnetization are frozen.

For the  $XXZ$  model ( $J_z \neq J_x = J_y \equiv J$ ), the time-dependent coefficients  $\sigma_\alpha(t)$  of Eqs. (2.13) are the harmonic oscillations (2.8). The general solution can be obtained by standard methods and is given in Ref. 11, Eqs. (3). The motion of the  $S_i(t)$  is again harmonic, now characterized by the two independent frequencies

$$\Omega_z = (J - J_z)\sigma_z, \quad \bar{\Omega} = J\sigma. \quad (2.14)$$

In the general  $XYZ$  model, the time-dependent coefficients  $\sigma_\alpha(t)$  entering Eqs. (2.13) are given by the anharmonic oscillations (2.9). The motion of the individual spins  $S_i(t)$  is then still characterized by two fundamental frequencies, one of which is (2.11), but the associated intensity spectra now include lines at their multiples, sums, and differences.

### C. Distribution functions

For the direct evaluation of the dynamic spin correlation functions in Sec. III, we need to know not only the rotational motion of  $\sigma(t)$  for given initial values, but also the distribution of initial values, specifically the joint probability distributions  $P(\sigma, \sigma_z)$  ( $XXZ$  model) or  $P(\sigma, \epsilon)$  ( $XYZ$  model) of the two integrals of the motion which guarantee the integrability of the effective two-spin system ( $\sigma, S_i$ ). For a canonical ensemble at  $T = \infty$ , these distributions are readily determined by an application of the central limit theorem. The distribution function for any Cartesian component  $S_i^\alpha$  of an individual spin is rectangular,

$$P_1(S_i^\alpha) = \frac{1}{2}\Theta(1 - |S_i^\alpha|), \quad (2.15)$$

with variance  $\langle (S_i^\alpha)^2 \rangle = \frac{1}{3}$ . In the absence of any instantaneous correlations between individual spins, the distribution of the collective-spin variable  $\sigma_\alpha$  is then a Gaussian with the same variance,

$$P_\alpha(\sigma_\alpha) = C \exp(-3\sigma_\alpha^2/2), \quad C \equiv \sqrt{3/2\pi}, \quad (2.16)$$

and the distribution function for the length of  $\sigma$  is a Maxwellian,

$$P(\sigma) = 4\pi C^3 \sigma^2 \exp(-3\sigma^2/2). \quad (2.17)$$

These distributions are model independent. Note that the collective spin has the same mean-square length  $\langle \sigma^2 \rangle = 1$  as the fixed-length individual spin. For the  $XXZ$  model, the joint probability distribution  $P(\sigma, \sigma_z)$  can be constructed from (2.17) and the conditional probability distribution

$$P(\sigma_z | \sigma) = \frac{1}{2\sigma} \Theta(\sigma - |\sigma_z|) \quad (2.18)$$

via the relation  $P(\sigma, \sigma_z) = P(\sigma_z | \sigma)P(\sigma)$  as

$$P(\sigma, \sigma_z) = 2\pi C^3 \sigma \exp(-3\sigma^2/2) \Theta(\sigma - |\sigma_z|). \quad (2.19)$$

In the general  $XYZ$  model,  $\sigma_z$  is no longer conserved and must be replaced by the energy  $\epsilon = |\bar{H}|$  as defined in (2.6). The same argument then yields an explicit expression for  $P(\sigma, \epsilon)$ .

### III. DYNAMIC CORRELATION FUNCTIONS AND SPECTRAL DENSITIES

Given the explicit solutions for the dynamical variables  $\sigma_\alpha(t)$  and  $S_i^\alpha(t)$  pertaining to arbitrary initial conditions, and given the joint distribution functions for the invariants which specify individual solutions, it is then possible, at least in principle, to evaluate dynamic correlation functions for these variables directly. In this section we pursue this road to the extent that we find it practical, viz., for the  $XXZ$  model. An alternative approach, the recursion method, is taken in Sec. IV for the general  $XYZ$  case.

#### A. Collective-spin autocorrelation functions for the $XXZ$ model

For  $J_x = J_y \equiv J$ , it is straightforward to evaluate the functions  $\langle \sigma_\alpha(t) \sigma_\alpha \rangle$  from the exact solution (2.8). In the expression

$$\langle \sigma_x(t) \sigma_x \rangle = \frac{1}{2} \langle (\sigma^2 - \sigma_z^2) \cos(\Omega_z t) \rangle, \quad (3.1)$$

we have already performed a time average over one period of the dynamical variable. The ensemble average

$$\begin{aligned} 3\langle S_i^x(t) S_i^x \rangle &= \frac{J_z}{J_z - J} \exp(-\frac{1}{6} J_z^2 t^2) + \frac{3}{(J - J_z)^2 t^2} [\exp(-\frac{1}{6} J_z^2 t^2) - \exp(-\frac{1}{6} (J - J_z)^2 t^2)] \\ &\quad + \frac{3\pi C}{(J - J_z)^3 t^3} \left[ \operatorname{erf} \left( \frac{J - J_z}{\sqrt{6}} t \right) - \frac{1}{2} \operatorname{erf} \left( \frac{2J - J_z}{\sqrt{6}} t \right) + \frac{1}{2} \operatorname{erf} \left( \frac{J_z}{\sqrt{6}} t \right) \right], \end{aligned} \quad (3.6a)$$

$$3\langle S_i^z(t) S_i^z \rangle = \frac{1}{3} + \frac{2}{3} (1 - \frac{1}{3} J^2 t^2) \exp(-J^2 t^2/6); \quad (3.6b)$$

$$\begin{aligned} \Phi_0^{xx}(\omega)_S &= \frac{\pi^2 C^3}{|J - J_z|} \left[ \frac{2}{3} \exp \left( -\frac{3}{2} \frac{\omega^2}{(J - J_z)^2} \right) + \frac{\omega^2}{(J - J_z)^2} \operatorname{Ei} \left( -\frac{3}{2} \frac{\omega^2}{(J - J_z)^2} \right) \right. \\ &\quad \left. + \frac{1}{3} \frac{2J - J_z}{J - J_z} \left| \frac{2J - J_z}{J - J_z} \right| \left[ \exp \left( -\frac{3}{2} \frac{\omega^2}{(2J - J_z)^2} \right) - \operatorname{sgn}(2J - J_z) \exp \left( -\frac{3}{2} \frac{\omega^2}{J_z^2} \right) \right] \right] \\ &\quad - \frac{(2J - J_z)/C}{(J - J_z)|J - J_z|} |\omega| \left\{ \left| \operatorname{erf} \left[ \left( \frac{3}{2} \right)^{1/2} \frac{\omega}{J_z} \right] \right| - \left| \operatorname{erf} \left[ \left( \frac{3}{2} \right)^{1/2} \frac{\omega}{2J - J_z} \right] \right| \right\} \\ &\quad + \frac{1}{2} \frac{\omega^2}{(J - J_z)|J - J_z|} \left[ \operatorname{Ei} \left( -\frac{3}{2} \frac{\omega^2}{J_z^2} \right) - \operatorname{sgn}(2J - J_z) \operatorname{Ei} \left( -\frac{3}{2} \frac{\omega^2}{(2J - J_z)^2} \right) \right], \end{aligned} \quad (3.7a)$$

is completed by averaging over the invariants  $\sigma$  and  $\sigma_z$ , using the joint probability distribution (2.19). The result is a pure Gaussian:

$$3\langle \sigma_x(t) \sigma_x \rangle = \exp[-\frac{1}{6} (J - J_z)^2 t^2]. \quad (3.2)$$

The associated spectral density

$$\Phi_0^{xx}(\omega)_\sigma \equiv \int_{-\infty}^{+\infty} dt e^{i\omega t} \frac{\langle \sigma_x(t) \sigma_x \rangle}{\langle \sigma_x \sigma_x \rangle} \quad (3.3)$$

is then also a pure Gaussian:

$$\Phi_0^{xx}(\omega)_\sigma = \frac{2\pi C}{|J - J_z|} \exp[-\frac{3}{2} \omega^2 / (J - J_z)^2]. \quad (3.4)$$

In (3.4) the width of the spectra-weight distribution goes to zero if  $J - J_z \rightarrow 0$ , which is consistent with the fact that  $\sigma_x$  is conserved in the  $XXX$  case. Naturally, we have  $\langle \sigma_z(t) \sigma_z \rangle = \frac{1}{3}$  for all  $XXZ$  cases.

#### B. Single-spin autocorrelation functions for the $XXZ$ model

The evaluation of the single-spin autocorrelation functions  $\langle S_i^\alpha(t) S_i^\alpha \rangle$  for  $J_x = J_y \equiv J$  proceeds along the same lines, but there are some complications.<sup>11</sup> Performing the time average of  $S_i^\alpha(t) S_i^\alpha(0)$  over a single orbit followed by a partial ensemble average yields the expressions

$$\begin{aligned} \langle S_i^x(t) S_i^x \rangle &= \frac{1}{6} \left\langle \frac{\sigma^2 - \sigma_z^2}{\sigma^2} \cos(\Omega_z t) \right\rangle \\ &\quad + \frac{1}{6} \left\langle \frac{(\sigma - \sigma_z)^2}{\sigma^2} \cos[(\bar{\Omega} + \Omega_z)t] \right\rangle, \end{aligned} \quad (3.5a)$$

$$\langle S_i^z(t) S_i^z \rangle = \frac{1}{3} \left\langle \frac{\sigma^2 - \sigma_z^2}{\sigma^2} \cos(\bar{\Omega} t) \right\rangle + \frac{1}{3} \left\langle \frac{\sigma_z^2}{\sigma^2} \right\rangle, \quad (3.5b)$$

which depend only on the invariants  $\sigma$  and  $\sigma_z$  in addition to  $t$ . Using (2.19) for the remaining ensemble average, we obtain the following closed-form results for the single-spin autocorrelation functions and their spectral densities:

$$\Phi_0^{zz}(\omega)_S = C^{-2}\delta(\omega) + \frac{4\pi C\omega^2}{J^3} \exp\left(-\frac{3}{2}\frac{\omega^2}{J^2}\right). \quad (3.7b)$$

A peculiar property of the function  $\Phi_0^{zz}(\omega)_S$  is its independence of  $J_z$ . The associated spin autocorrelation function (3.6b) decays like a Gaussian to a nonzero constant. The spectral density  $\Phi_0^{xx}(\omega)_S$ , by contrast, does depend on the uniaxial anisotropy. For  $J=0$ , expression (3.7a) reduces to a simple Gaussian,

$$\Phi_0^{xx}(\omega)_S = (2\pi C/J_z) \exp(-3\omega^2/2J_z^2), \quad (3.8)$$

and (3.6a) reduces to  $3\langle S_i^x(t)S_i^x \rangle = \exp(-J_z^2 t^2/6)$ . In fact, the long-time asymptotic decay of  $\langle S_i^x(t)S_i^x \rangle$  is Gaussian throughout the regime  $J_z > 2J$  of easy-axis anisotropy. In the regime  $0 < J_z < 2J$ ,  $J_z \neq J$ , the spectral density  $\Phi_0^{xx}(\omega)_S$  has a singularity at  $\omega=0$  of the form  $\sim \omega^2 \ln(\omega)$ , which implies that the correlation function decays algebraically for long times  $\langle S_i^x(t)S_i^x \rangle \sim t^{-3}$ . In the limit  $J_z=0$ , a stronger singularity makes its appearance,  $\sim |\omega|$ , implying a slower long-time asymptotic decay of the associated correlation function  $\langle S_i^x(t)S_i^x \rangle \sim t^{-2}$ .

Figure 1 shows the spectral density  $\Phi_0^{xx}(\omega)_S$  for several cases of the XXZ model. Starting out with the Gaussian (3.8) in the limit  $J=0$  ( $g=0$ ) and increasing  $J$  relative to  $J_z$ , we observe that the peak at  $\omega=0$  becomes higher and narrower, while a second peak at nonzero  $\omega$  emerges. In the XXX limit ( $J=J_z$ ,  $g=0.25$ ), the peak at  $\omega=0$  diverges and turns into a  $\delta$  function, described by expression (3.7b). As  $J_z$  decreases below  $J$ , the  $\delta$  function at  $\omega=0$  transforms back into a peak of diminishing height ( $g=0.3$  and inset), the maximum at  $\omega=0$  turns into a

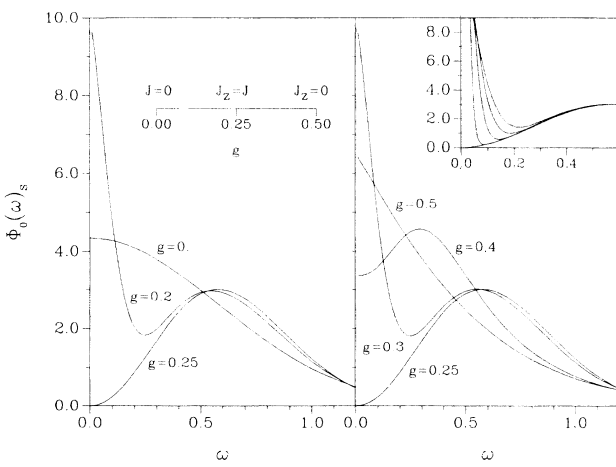


FIG. 1. Spectral density  $\Phi_0^{xx}(\omega)_S$  of the classical equivalent-neighbor XXZ model at  $T=\infty$ . The curves represent the exact result (3.7a) for six different values of uniaxial anisotropy, here parametrized as  $J=\sin(\pi g)$ ,  $J_z=\cos(\pi g)$ . The inset shows the same function for parameter values  $g=0.29, 0.28, 0.27, 0.26$ , approaching the XXX model ( $g=0.25$ ), for which case (3.7a) reduces to (3.7b).

minimum ( $g=0.4$ ), and the smooth peak at nonzero  $\omega$  gradually moves towards lower frequencies; in the limit  $J_z=0$  ( $g=0.5$ ), it turns into a cusp singularity at  $\omega=0$ .

Note that the decay of the XXZ model spectral densities for large  $\omega$  is always Gaussian in character, independent of the amount of uniaxial anisotropy. In Sec. V such behavior will be interpreted as a consequence of the linear dynamics of that model, and we shall demonstrate that the nonlinear dynamics of the XYZ model leads to a different decay law. For the analysis of this particular aspect of dynamical behavior, the recursion method presents itself as a convenient computational tool.

#### IV. RECURSION METHOD

For applications to dynamical problems, the recursion method<sup>12</sup> is a modern version of the projection operator technique designed by Mori and Zwanzig, reformulated to make it directly accessible to computational methods. It is applicable with equal ease to models with linear and nonlinear dynamics, to integrable and nonintegrable models, to classical and quantum models. For applications to  $T=\infty$  spin dynamics, we shall employ the formulation of the recursion method developed some years ago by Lee.<sup>13</sup>

##### A. Formulation for classical spin dynamics

Given a dynamical system specified by some energy function  $H(\mathbf{S}_1, \dots, \mathbf{S}_N)$  and the symplectic structure for classical spins,

$$\{S_i^\alpha, S_j^\beta\} = \delta_{ij} \sum_\gamma \epsilon_{\alpha\beta\gamma} S_i^\gamma, \quad (4.1)$$

the time evolution of any dynamical variable  $G(\mathbf{S}_1, \dots, \mathbf{S}_N)$  is governed by Hamilton's equation of motion,

$$\frac{dG}{dt} = \{G, H\} = iLG, \quad (4.2)$$

where  $L=i\{H, \cdot\}$  is the classical Liouville operator expressed as a Poisson bracket. The formulation of the recursion method for the autocorrelation function  $\langle G(t)G(0) \rangle$  is based on an orthogonal expansion of the dynamical variable under scrutiny:

$$G(t) = \sum_{k=0}^{\infty} A_k(t) f_k. \quad (4.3)$$

The orthogonal vectors  $f_k$  are generated recursively via the Gram-Schmidt orthogonalization procedure with initial condition  $f_0 = G(0)$ ,  $f_{-1} \equiv 0$ :

$$f_{k+1} = iLf_k + \Delta_k f_{k-1}, \quad k=1, 2, \dots, \quad (4.4)$$

$$\Delta_k = (f_k, f_k) / (f_{k-1}, f_{k-1}). \quad (4.5)$$

The inner product used in (4.5) is defined as the canonical average,

$$\langle AB \rangle = \langle AB \rangle = \frac{1}{Z} \int d^N q \, d^N p \, e^{-\beta H(q,p)} A(q,p) B(q,p), \quad (4.6)$$

where  $\beta=1/k_B T$  and  $Z$  is the classical partition function. For classical spins,

$$\mathbf{S}_i = (S_i^x, S_i^y, S_i^z) = (\sin \vartheta_i \cos \varphi_i, \sin \vartheta_i \sin \varphi_i, \cos \vartheta_i), \quad (4.7)$$

the phase manifold is a product of unit spheres and a pair of canonical coordinates for  $\mathbf{S}_i$  are  $p_i = \cos \vartheta_i$ ,  $q_i = \varphi_i$ .

For energy functions  $H(\mathbf{S}_1, \dots, \mathbf{S}_N)$  with a XYZ-type bilinear (not necessarily equivalent-neighbor) interaction, all nonvanishing inner products are multispin equal-time correlation functions. At  $T=\infty$  they conveniently factorize, and each factor can be evaluated in closed form:

$$\begin{aligned} & \langle (S_i^x)^{2\kappa_x} (S_i^y)^{2\kappa_y} (S_i^z)^{2\kappa_z} \rangle \\ &= \frac{(2\kappa_x - 1)!!(2\kappa_y - 1)!!(2\kappa_z - 1)!!}{(2\kappa_x + 2\kappa_y + 2\kappa_z + 1)!!}. \end{aligned} \quad (4.8)$$

The sequence of recurrents  $\Delta_k$ , if indeed known, contains all the information necessary to reconstruct the autocorrelation function  $\langle G(t)G(0) \rangle$  as follows. We insert the orthogonal expansion (4.3) into the equation of motion (4.2) to obtain a set of linear differential equations for the coefficients  $A_k(t)$ :

$$\dot{A}_k(t) = A_{k-1}(t) - \Delta_{k+1} A_{k+1}(t), \quad k = 0, 1, 2, \dots \quad (4.9)$$

with  $A_{-1}(t) \equiv 0$ ,  $A_k(0) = \delta_{k,0}$ , and where

$$A_0(t) = \frac{\langle G(t), G(0) \rangle}{\langle G(0), G(0) \rangle} = \frac{\langle G(t)G(0) \rangle}{\langle G^2 \rangle} \quad (4.10)$$

is the (normalized) autocorrelation function we wish to determine. Equation (4.9), converted by Laplace transform into a set of algebraic equations,

$$\begin{aligned} za_k(z) - \delta_{k,0} &= a_{k-1}(z) - \Delta_{k+1} a_{k+1}(z), \\ k &= 0, 1, 2, \dots \end{aligned} \quad (4.11)$$

with  $a_{-1}(z) \equiv 0$ , can be solved for the relaxation function  $a_0(z)$  in the continued-fraction representation:

$$a_0(z) \equiv \int_0^\infty dt e^{-zt} A_0(t) = \frac{1}{z + \frac{\Delta_1}{z + \frac{\Delta_2}{z + \dots}}}. \quad (4.12)$$

The spectral density is obtained from (4.12) via the relation

$$\Phi_0(\omega) \equiv \int_{-\infty}^{+\infty} dt e^{i\omega t} A_0(t) = 2 \operatorname{Re} \lim_{\epsilon \rightarrow 0} a_0(\epsilon - i\omega). \quad (4.13)$$

In the absence of any method by which time-dependent spin correlation functions and their spectral densities for a given model system can be evaluated on a rigorous basis, the recursion method can be employed to reconstruct a more or less accurate approximation of the spectral density. In most practical applications of the recursion method, only a limited number of recurrences  $\Delta_n$  can be determined. This makes it necessary to terminate the continued fraction (4.12) artificially. A simple but quite powerful procedure to do this was presented in Ref. 14. Here we shall focus on information which can be extracted directly from the  $\Delta_n$  sequence.

## B. Application to the equivalent-neighbor XYZ model

In Sec. II we have shown how the many-body dynamics of the classical equivalent-neighbor XYZ model, which is intractably complicated for finite  $N$ , turns effectively into a physical ensemble of nonlinear two-degrees-of-freedom Hamiltonian systems as  $N \rightarrow \infty$ . That transformation can be exploited to increase the computational efficiency of the recursion method significantly and to clarify the relation between the dynamics of the classical and the quantum equivalent-neighbor XYZ models.

We rewrite the classical energy function (2.1) in the form

$$H = -\frac{1}{2\sqrt{N}} \sum_{\alpha=xyz} J_\alpha M_\alpha M_\alpha + \frac{1}{2\sqrt{N}} \sum_{\alpha=xyz} \sum_{i=1}^N J_\alpha (S_i^\alpha)^2, \quad (4.14)$$

where

$$M_\alpha = \sum_{i=1}^N S_i^\alpha, \quad \alpha = x, y, z. \quad (4.15)$$

The Poisson brackets for the two sets of variables  $S_i^\alpha$  and  $M_\alpha$  are

$$\begin{aligned} \{S_i^\alpha, S_j^\beta\} &= \delta_{ij} \sum_\gamma \epsilon_{\alpha\beta\gamma} S_i^\gamma, \\ \{S_i^\alpha, M_\beta\} &= \sum_\gamma \epsilon_{\alpha\beta\gamma} S_i^\gamma, \\ \{M_\alpha, M_\beta\} &= \sum_\gamma \epsilon_{\alpha\beta\gamma} M_\gamma. \end{aligned} \quad (4.16)$$

In the recursion method, as applied to the spin autocorrelation functions  $\langle S_i^\alpha(t) S_i^\alpha \rangle$ , all inner products to be evaluated have the following general structure:

$$(f_n, f_n) = N^{-n} (b_n N^n + b_{n-1} N^{n-1} + \dots + b_0). \quad (4.17)$$

Hence all terms except the leading ( $N$ -independent) one represent finite-size corrections. It turns out that only the  $M_\alpha$  terms in (4.14) contribute to the dynamics of the infinite system. Any surviving contribution to the vector  $f_n$  in the orthogonal expansion (4.3) has the general form

$$N^{-(m_x + m_y + m_z)/2} S_i^\alpha (M_x)^{m_x} (M_y)^{m_y} (M_z)^{m_z}. \quad (4.18)$$

All nonvanishing inner products, expanded in inverse powers of  $N$ , factorize to leading order:

$$\begin{aligned} & \langle (S_i^\alpha)^2 \prod_{\gamma=xyz} N^{-m_\gamma} M_\gamma^{2m_\gamma} \rangle \\ &= \langle (S_i^\alpha)^2 \rangle \prod_{\gamma=xyz} N^{-m_\gamma} \langle M_\gamma^{2m_\gamma} \rangle [1 + O(N^{-1})], \end{aligned} \quad (4.19)$$

with

$$N^{-m_\alpha} \langle M_\alpha^{2m_\alpha} \rangle = 3^{-m_\alpha} (2m_\alpha - 1)!! [1 + O(N^{-1})]. \quad (4.20)$$

Exactly the same inner products are obtained from a physical ensemble of the two-degrees-of-freedom system

discussed in Sec. II. That system consists of a spin  $S_i$  of unit length coupled parasitically (i.e., with no dynamical feedback) to an autonomous single-spin system, a spin  $\sigma$  of unit rms length driven by the Hamiltonian (2.6). The distributions (2.15) and (2.16) yield precisely the right expectation values,

$$\langle (S_i^\alpha)^2 \rangle = \frac{1}{3}, \quad \langle \sigma_{\alpha}^{2m_\alpha} \rangle = (2m_\alpha - 1)!! / 3^{m_\alpha}, \quad (4.21)$$

to simulate the many-body dynamics.

In our computational implementation of the recursion method the goal is to determine the longest possible  $\Delta_n$  sequences of single-spin and collective-spin autocorrelation functions for further analysis as described in Sec. V. For finite  $N$ , the input consists of the  $N$ -body Hamiltonian (2.1), the initial condition  $f_0 = S_i^\alpha$ , and the expectation values (4.8) for the evaluation of inner products. For  $N = \infty$  the input consists of the single-spin Hamiltonian (2.6), the initial conditions  $f_0 = S_i^\alpha$  or  $f_0 = \sigma_\alpha$ , and the expectation values (4.21). For each of the two situations we have constructed a computer program which evaluates the recurrants sequentially according to the rules of the recursion method.

### C. Quantum equivalent-neighbor XYZ model

Through minor modifications, the recursion method can be adapted to the dynamics of the quantum equivalent-neighbor XYZ model, which is specified by the Hamiltonian (2.1) or (4.14) with the  $S_i$  now representing spin- $s$  operators. We substitute the quantum Liouville operator  $L = [H, ]$  (commutator) into the equation of motion (4.2), replace the symplectic structure (4.1) by the commutator algebra for quantum spins  $[S_i^\alpha, S_j^\beta] = i\delta_{ij}\sum_\gamma \epsilon_{\alpha\beta\gamma} S_i^\gamma$ , and use (for  $T = \infty$  only) the inner product  $(A, B) = \text{Tr}(AB)$ . In spite of the structural similarity of the elements which go into the classical and quantum versions of the recursion method, the resulting dynamics is, in general, quite different for the two cases.

However, the equivalent-neighbor XYZ model is atypical in this respect. All inner products have the general structure (4.17) in both the quantum and the classical cases, and the dynamics of the infinite system is determined by the leading term alone. The important point to note is that all terms in  $f_n$  which contribute to leading order in (4.17) contain commuting operators only, specifically operators pertaining to different sites of the array. The net result is that the recurrants  $\Delta_n$  of  $\langle S_i^\alpha(t)S_i^\alpha \rangle$  for the infinite quantum equivalent-neighbor XYZ model differ from those of its classical counterpart only by a multiplicative constant (which depends on  $s$ ), amounting to a different time scale in the dynamical correlation functions. This explains the observation that our results for dynamic correlation functions of the classical equivalent-neighbor XXZ model presented in Sec. III are fully consistent with the results previously obtained by Lee, Dekeyser, and Kim<sup>15,16</sup> for the quantum spin- $\frac{1}{2}$  counterpart of that model.<sup>17</sup> Finite-size effects are, however, dramatically different in the quantum and classical cases.

### V. GROWTH RATE OF $\Delta_n$ SEQUENCES

The growth rate of the  $\Delta_n$  sequence for a dynamic correlation function as obtained by the recursion method is defined as the exponent  $\lambda$  characterizing the average power-law growth

$$\Delta_n \sim n^\lambda \quad (5.1)$$

asymptotically for large  $n$ . The complete  $\Delta_n$  sequence is necessary to fully determine any dynamic correlation function, but its growth rate alone determines the type of decay of the associated spectral density

$$\Phi_0(\omega) \sim \exp(-\omega^{2/\lambda}) \quad (5.2)$$

asymptotically for large  $\omega$ .<sup>18</sup> The point we wish to emphasize here is that the growth rate of  $\Delta_n$  sequences can be used to characterize universality classes of dynamical behavior similar to the usage of that term in the theory of critical phenomena. The  $T = \infty$  dynamics of the equivalent-neighbor XYZ model provides realizations for the universality classes corresponding to integer-valued exponents  $\lambda = 0, 1, 2, 3$ , as will be demonstrated in the following.

In integrable classical dynamical systems, the growth rate of the  $\Delta_n$  sequences for specific autocorrelation functions is basically dominated by two factors.

(a) This factor depends on whether the equations of motion are linear or nonlinear. Each harmonic mode contributes exactly one  $\delta$  function to the spectral density (at  $\omega > 0$ ), whereas each anharmonic mode contributes an infinite set of  $\delta$  functions, at frequencies with no upper bound. In nonlinear systems, factor (a) is governed by the large- $\omega$  decay law of the line intensities for single modes.

(b) This factor is governed by the distribution of fundamental frequencies pertaining to individual linear or nonlinear modes. That distribution depends sensitively on whether the size of the system is finite or infinite and (for infinite systems) on whether the interaction range is finite or infinite.

The effect of each factor on the large- $\omega$  decay law of the spectral density is expressible in terms of a distribution function: factor (a) by the spectral-weight distribution  $P_n(n)$  of individual modes and factor (b) by the distribution  $P_\Omega(\Omega)$  of fundamental frequencies of these modes. The large- $\omega$  decay law of the spectral density is then obtained from these distributions by the following construction:

$$\Phi_0(\omega) \sim \int_0^\infty d\Omega P_\Omega(\Omega) \int_0^\infty dn P_n(n) \delta(\omega - n\Omega). \quad (5.3)$$

For distributions with asymptotic decay laws of the form

$$P_n(n) \sim \exp(-n^\alpha), \quad P_\Omega(\Omega) \sim \exp(-\Omega^\beta), \quad (5.4)$$

the large- $\omega$  decay law of the resulting spectral density as obtained from (5.3) is given by (5.2) with exponent

$$\lambda(\alpha, \beta) = 2(\alpha + \beta)/\alpha\beta. \quad (5.5)$$

In the context of the classical equivalent-neighbor XYZ model, factors (a) and (b) produce a total of four different

TABLE I. Large- $\omega$  asymptotic decay law of the spectral density  $\Phi_0(\omega)$  and growth rate  $\lambda$  of the associated  $\Delta_n$  sequence for the four different universality classes of dynamical behavior realized in the classical equivalent-neighbor  $XYZ$  model. The four classes arise as the product of the two factors (a) and (b), each represented by a distribution for which there are two distinct realizations.

Factor (a)		Factor (b)			
Dynamics	$P_n(n)$	Size of system	$P_\Omega(\Omega)$	$\Phi_0(\omega)$	$\lambda$
linear	$\delta(n-1)$	finite	compact support	compact support	0
nonlinear	$\delta(n-1)$	infinite	$\sim \exp(-\Omega^2)$	$\sim \exp(-\omega^2)$	1
	$\sim \exp(-n)$		compact support	$\sim \exp(-\omega)$	2
nonlinear	$\sim \exp(-n)$	infinite	$\sim \exp(-\Omega^2)$	$\sim \exp(-\omega^{2/3})$	3

decay laws of spectral densities, characterized by four different integer-valued growth rates  $\lambda$  of the associated  $\Delta_n$  sequences. These four universality classes of dynamical behavior are summarized in Table I. They can be identified as the special or limiting cases  $\lambda(\infty, \infty)=0$ ,  $\lambda(\infty, 2)=1$ ,  $\lambda(1, \infty)=2$ , and  $\lambda(1, 2)=3$ . In the following, we discuss realizations of each case.

#### A. Compact support ( $\lambda=0$ )

Quite generally,  $\Delta_n$  sequences with zero growth rate are realized in linear dynamical systems with a finite number of degrees of freedom. The finite- $N$   $XXX$  case is such a system as is evident from our discussion in Sec. II B. Consider the spin autocorrelation function  $A_0(t) \equiv \langle \mathbf{S}_i(t) \cdot \mathbf{S}_i \rangle$  for the two-spin  $XXX$  case with  $\bar{J}=J/\sqrt{2}$ . The exact result reads:<sup>19,20</sup>

$$A_0(t) = \frac{1}{2} + \frac{3}{2(\bar{J}t)^3} \sin(2\bar{J}t) - \frac{3+2(\bar{J}t)^2}{4(\bar{J}t)^4} + \frac{3-4(\bar{J}t)^2}{4(\bar{J}t)^4} \cos(2\bar{J}t), \quad (5.6)$$

and its spectral density

TABLE II. First 12 recurrents  $\Delta_n$  for the spin autocorrelation function  $\langle \mathbf{S}_i(t) \cdot \mathbf{S}_i \rangle$  at  $T=\infty$  of the classical two-spin model  $H=-\bar{J}\mathbf{S}_1 \cdot \mathbf{S}_2$  as determined computationally by the recursion method. Also given is the number (No.) of distinct terms of the form  $\prod_{i=1}^2 \prod_{\alpha=x,y,z} (S_i^\alpha)^{m_\alpha}$ , which make up the vector  $f_n$  in the orthogonal expansion (4.31).

$n$	$\Delta_n/\bar{J}^2$	No.	$n$	$\Delta_n/\bar{J}_n^2$	No.
1	$\frac{2}{3}$	2	2	$\frac{4}{3}$	9
3	$\frac{3}{5}$	20	4	$\frac{7}{5}$	61
5	$\frac{32}{49}$	98	6	$\frac{66}{49}$	243
7	$\frac{70}{99}$	340	8	$\frac{128}{99}$	707
9	$\frac{3}{4}$	944	10	$\frac{5}{4}$	1775
11	$\frac{112}{143}$	2244	12	$\frac{174}{143}$	3891

$$\Phi_0^{\alpha\alpha}(\omega)_S = \pi\delta(\omega) + \frac{\pi}{8}|\omega|(4\bar{J}^2 - \omega^2)\Theta(2\bar{J} - |\omega|) \quad (5.7)$$

has indeed compact support. The trend of the  $\Delta_n$  sequence as determined by the recursion method is to converge to the value  $\bar{J}^2$  in an alternating approach. See Table II for the first 12 recurrents as derived from the recursion method. If we consider instead of  $A_0(t)$  the function

$$\tilde{A}_0(t) \equiv \frac{A_0(t) - A_0(\infty)}{A_0(0) - A_0(\infty)}, \quad (5.8)$$

its  $\Delta_n$  sequence can be expressed in closed form as

$$\Delta_{2n} = \bar{J}^2 \left[ 1 - \frac{1}{2n+1} \right], \quad \Delta_{2n-1} = \bar{J}^2 \left[ 1 + \frac{1}{2n+1} \right]. \quad (5.9)$$

Let us introduce the sequence

$$\Lambda_n = (\Delta_{2n-1} + \Delta_{2n})/2, \quad (5.10)$$

which represents partial information on the spectral density. It is useful to note that the two functions  $A_0(t)$  and  $\tilde{A}_0(t)$ , whose spectral densities differ by an additive  $\delta$ -function term at  $\omega=0$ , are characterized by the same  $\Lambda_n$  sequence (in this case  $\Lambda_n = \bar{J}^2$ ), but different  $\Delta_n$  sequences.

The situation here is represented by the first row of Table I and by the limiting case  $(\alpha, \beta)=(\infty, \infty)$  of Eqs. (5.3)–(5.5). For the  $XXX$  case with  $N > 2$  but finite, the  $\Delta_n$  sequence of  $A_0(t)$  exhibits a more complicated pattern, but still converges to a finite value  $\Delta_\infty = NJ^2/4$ , and the spectral density is bounded to  $|\omega| < \sqrt{NJ}$ . In the limit  $N = \infty$ , the growth rate of  $\Delta_n$  switches from  $\lambda=0$  to 1 as will be discussed next.

#### B. Gaussian decay ( $\lambda=1$ )

$\Delta_n$  sequences with linear growth rate ( $\lambda=1$ ) are common in many-body systems with linear dynamics. In the context of the infinite- $N$   $XXZ$  case, the Gaussian decay of the spectral densities (3.4) and (3.7) arises, via factor (b), from linear modes with a Gaussian frequency distribu-

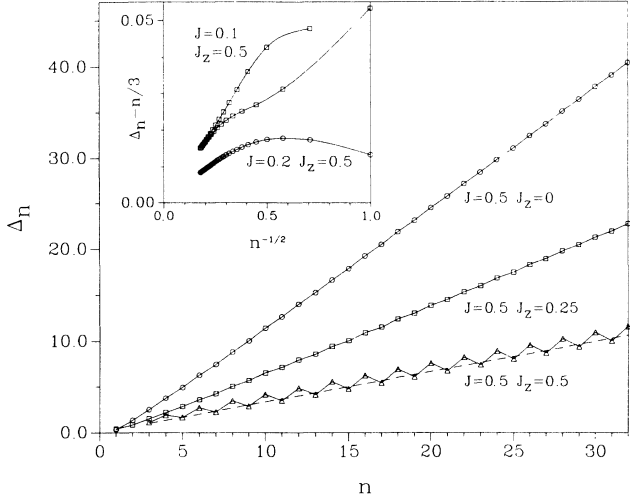


FIG. 2. Sequence of recurrents  $\Delta_n$  vs  $n$  for the single-spin autocorrelation function  $\langle S_i^x(t)S_i^x \rangle$  at  $T=\infty$  of the infinite- $N$  classical equivalent-neighbor XXZ model for three different sets of parameter values. For  $0 < J \leq J_z \equiv 1$ , the  $\Delta_n$  sequences oscillate about the (dashed) line  $n/3$ . The inset shows the deviations  $\Delta_n - n/3$  vs  $1/\sqrt{n}$  for two cases in which the oscillations die out as  $n \rightarrow \infty$ .

tion, a property dictated by the central limit theorem.

For the simplest realization of  $\lambda=1$ , consider the collective-spin autocorrelation function  $\langle \sigma_x(t)\sigma_x \rangle$ , whose spectral density is a pure Gaussian, given by (3.4) and characterized by the purely linear sequence  $\Delta_n = (J - J_z)^2 n / 3$ . This situation is represented by the second row of Table I and described by Eqs. (5.3)–(5.5) with  $(\alpha, \beta) = (\infty, 2)$ .

The growth rate  $\lambda=1$  is also realized in the single-spin autocorrelation functions  $\langle S_i^\alpha(t)S_i^\alpha \rangle$ , whose spectral densities, given by expressions (3.7), all exhibit Gaussian decay at high frequencies. In Fig. 2 we show several  $\Delta_n$  sequences (plotted versus  $n$ ) for  $\langle S_i^x(t)S_i^x \rangle$  at various values of  $J$  and  $J_z$ , all of which show indeed linear growth rate,

TABLE III. First 12 recurrents  $\Delta_n$  for the single-spin autocorrelation function  $\langle S_i(t) \cdot S_i \rangle$  at  $T=\infty$  of the equivalent-neighbor XXX model in the limit  $N \rightarrow \infty$ , as determined computationally by the recursion method. Also given is the number (No.) of distinct terms of the form (4.18), which make up the vector  $f_n$  in the orthogonal expansion (4.3).

$n$	$\Delta_n/J^2$	No.	$n$	$\Delta_n/J^2$	No.
1	$\frac{2}{3}$	2	2	1	5
3	$\frac{10}{9}$	9	4	$\frac{17}{9}$	16
5	$\frac{28}{17}$	24	6	$\frac{137}{51}$	37
7	$\frac{306}{137}$	50	8	$\frac{1411}{411}$	71
9	$\frac{12056}{4233}$	90	10	$\frac{17575}{4233}$	121
11	$\frac{36686}{10545}$	147	12	$\frac{17063}{3515}$	190

but now with marked corrections. Only the sequence for  $J=0$  is purely linear,  $\Delta_n = n J_z^2 / 3$ , representing expression (3.8). Throughout the regime  $0 < J < J_z$  the  $\Delta_n$  oscillate about the line  $n J_z^2 / 3$  (shown dashed in Fig. 2). These oscillations persist as  $n \rightarrow \infty$  if  $J_z/2 < J < J_z$  and thus determine the singularity structure of the spectral density (3.7a) and the power-law long-time tail of the correlation function (3.6a). For  $0 < J < J_z/2$ , on the other hand, the oscillations damp out as  $n \rightarrow \infty$ , which is illustrated for two cases in the inset to Fig. 2. These  $\Delta_n$  sequences describe spectral densities with no power-law singularities and correlation functions with no power-law long-time tail.

The exact values of the first 12 recurrences for the special XXX case ( $J_z=J$ ) are given in Table III. We observe that this fairly complex  $\Delta_n$  sequence yields a very simple  $\Lambda_n$  sequence  $\Lambda_n = (4n+1)J^2/3$ , which suggests that, as in the example discussed in Sec. V A, the spectral density of  $\Phi_0^{xx}(\omega)_S$  consists of the sum of a  $\delta$  function at  $\omega=0$  and a function whose  $\Delta_n$  sequence has a simpler structure. This is confirmed by expression (3.7b). Its second term represents the special case ( $\omega_0^2 = 2J^2/3$ ,  $\mu=3$ ) of the function

$$\Phi_0(\omega) = \frac{2\pi}{\omega_0 \Gamma(\mu/2)} (\omega/\omega_0)^{\mu-1} e^{-(\omega/\omega_0)^2}, \quad (5.11)$$

whose  $\Delta_n$  sequence reads<sup>18</sup>

$$\Delta_{2n-1} = \omega_0^2(n-1+\mu/2), \quad \Delta_{2n} = \omega_0^2 n. \quad (5.12)$$

### C. Exponential decay ( $\lambda=2$ )

Consider the spin autocorrelation function  $\langle S_i^x(t)S_i^x \rangle$  for the XXZ case with  $N=2$ , specifically the two-spin model with  $J_z=0$ . For this case, the anharmonic motion of the spin components  $S_i^\alpha$  was analyzed for arbitrary initial conditions in a quite different context.<sup>10</sup> The solutions are expressible in terms of Jacobi elliptic functions. These functions have the property that their line intensities decay exponentially fast at high frequencies [factor (a)]. For finite systems, the distribution of fundamental frequencies has compact support [factor (b)]. This situation is represented by the third row of Table I and by Eqs. (5.3)–(5.5) with  $(\alpha, \beta) = (1, \infty)$ , yielding an exponentially decaying spectral density and a  $\Delta_n$  sequence with quadratic growth rate. Figure 3 shows a plot of  $\Delta_n$  versus  $n^2$  for the first 18 recurrences of this case as determined by our computational procedure. The observed growth rate is perfectly consistent with  $\lambda=2$ . We might add as a remark that a purely quadratic growth rate  $\Delta_n = a^2 n^2$  represents a “spectral density” of the form

$$\Phi_0(\omega) + (\pi/a) \operatorname{sech}(\pi\omega/2a). \quad (5.13)$$

### D. Stretched exponential decay ( $\lambda=3$ )

For realizations of this last universality class, consider the collective-spin autocorrelation function  $\langle \sigma_\alpha(t)\sigma_\alpha \rangle$  of the XYZ case with  $N=\infty$ , specifically the function  $\langle \sigma_y(t)\sigma_y \rangle$  for  $J_x=(1+\gamma)/2$ ,  $J_y=(1-\gamma)/2$ ,  $J_z=0$ , and

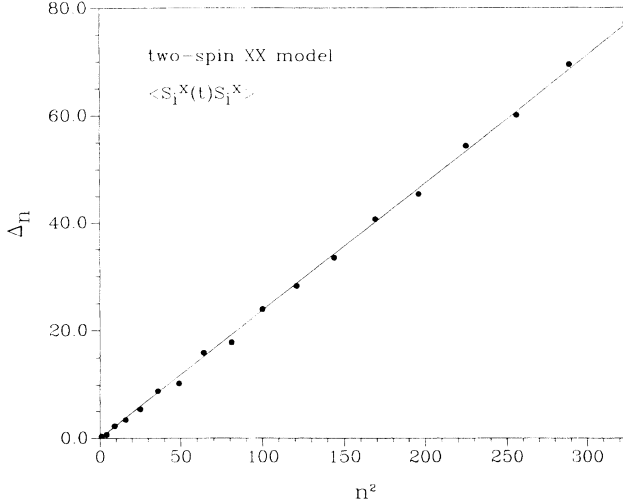


FIG. 3. Sequence of recurrents  $\Delta_n$  vs  $n^2$ ,  $n=1, \dots, 18$  for the spin autocorrelation function  $\langle S_i^x(t)S_i^x \rangle$  at  $T=\infty$  of the classical two-spin  $XX$  spin model,  $H=-(S_1^xS_2^x+S_1^yS_2^y)$ . The quadratic growth rate ( $\lambda=2$ ) for this function is demonstrated by the excellent fit of the regression line.

four different values of the parameter  $\gamma$ . For the two cases with uniaxial symmetry  $\gamma=0$  and 1, the dynamics is linear, whereas for the two intermediate cases with biaxial symmetry  $\gamma=\frac{1}{8}$  and  $\frac{3}{8}$ , it is nonlinear and describable in terms of Jacobi elliptic functions (see Sec. II A). In all of these cases, the distribution of fundamental frequencies of individual (linear or nonlinear) modes is characterized by a Gaussian decay [factor (b)], but for the nonlinear cases, the large- $\omega$  behavior of the spectral density is further governed by the exponential decay of line intensities at multiples of the fundamental frequencies [factor (a)]. These situations are represented, for the linear and nonlinear cases, respectively, by the second and fourth rows in Table I and by Eqs. (5.3)–(5.5) with exponent values  $(\alpha, \beta)$  equal to  $(\infty, 2)$  and  $(1, 2)$ . Figure 4 shows for the four specified cases  $\Delta_n$  versus  $n$  in a log-log plot as determined computationally by the recursion method. The switch from linear to nonlinear dynamics causes the growth rate to jump from  $\lambda=1$  to 3.

## VI. MANY-BODY SYSTEMS WITH SHORT-RANGE INTERACTION

The results of this study suggest that the four different universality classes of dynamical behavior observed in the context of the classical equivalent-neighbor  $XYZ$  model may serve as prototypes for a classification of the dynamics of general classical and quantum many-body systems. The exponent values  $\lambda=0, 1, 2, 3$ , which are realized in this somewhat artificial dynamical model, then play a role similar to the “classical” exponent values in the theory of phase transitions, which are also realized by the equivalent-neighbor model now interpreted as mean-field approximation to a thermodynamic system with short-range interactions.

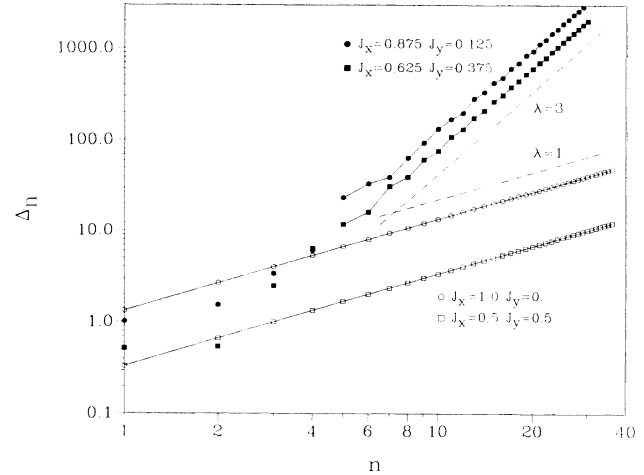


FIG. 4. Log-log plot of sequences  $\Delta_n$  vs  $n$  for the collective-spin autocorrelation function  $\langle \sigma_y(t)\sigma_y \rangle$  at  $T=\infty$  of the infinite- $N$  classical equivalent-neighbor  $XYZ$  model for four different sets of parameter values. The two cases with uniaxial symmetry (implying linear dynamics) yield linear growth rate ( $\lambda=1$ ), whereas the two cases with biaxial symmetry (implying nonlinear dynamics) yield cubic growth rate ( $\lambda=3$ ). Lines with slopes  $\lambda=1$  and 3 are shown by the dashed lines.

Studies of critical phenomena have convincingly demonstrated that the values of critical-point exponents of model systems with short-range interaction are determined by more subtle properties than is suggested by mean-field theory. Likewise, the growth rates that characterize dynamic correlation functions of many-body systems with short-range interactions call for an interpretation which transcends the classification used in Sec. V.

We wish to conclude this paper with a series of remarks, some factual, some tentative or speculative, whose main purpose it is to highlight some observations made on classical and quantum spin models with short-range interactions.<sup>21</sup>

(i) Dynamic correlation functions of generic quantum many-body systems appear to be characterized by  $\Delta_n$  sequences with growth rates in the vicinity of  $\lambda=1$ .

(ii) One of very few quantum many-body systems for which nontrivial dynamic correlation functions can be evaluated exactly is the one-dimensional (1D)  $s=\frac{1}{2}$   $XX$  model,

$$H = - \sum_{i=1}^N (S_i^x S_{i+1}^x + S_i^y S_{i+1}^y). \quad (6.1)$$

For that model, growth rates  $\lambda=1$  and 0 are both realized.<sup>14,22,23</sup> The former characterizes the correlation functions with the maximum degree of complexity for that model, while the latter occurs as a result of special circumstances which impose exceptionally stringent selection rules on transition rates.

(iii) For autocorrelation functions  $A_0(t)$  which are entire functions of (complex) time the growth rate  $\lambda$  of the  $\Delta_n$  sequence is expressible as  $\lambda=2(\rho-1)/\rho$  in terms of the growth order  $\rho$ . The latter quantity specifies the

growth of  $A_0(t)$  for large imaginary times:<sup>22</sup>  $A_0(i\tau) \sim \exp(\tau^\rho)$ . A proof that  $A_0(t)$  is entire exists only for 1D quantum systems with finite-range interaction.<sup>24</sup>

(iv) Some evidence for growth rates  $\lambda > 1$  in quantum many-body systems does exist, namely for the spin autocorrelation functions at  $T = \infty$  of the 1D  $s = \frac{1}{2}$   $XXX$  model (Heisenberg model). An extrapolation based on the analysis of the first 15 nonzero frequency moments (they determine the  $\Delta_n$  up to  $n = 15$ ) suggest a growth rate  $\lambda > 1.18$  for that case.<sup>22</sup> More systematic studies on quantum spin models are clearly called for.

(v) Dynamic correlation functions of generic classical many-body systems with short-range interactions and nonlinear dynamics appear to have growth rates in the vicinity of  $\lambda = 2$ . This is in marked contrast to their quantum counterparts [cf. remark (i)].

(vi) Figure 5 shows in juxtaposition the first seven recurrences  $\Delta_n$  versus  $n$  (in a log-log plot) for the spin autocorrelation function  $\langle S_i^x(t)S_i^x \rangle$  of the 1D classical  $XX$  model (6.1) and its quantum spin- $\frac{1}{2}$  counterpart. While the sequence of the quantum model is an exact realization of  $\lambda = 1$  [cf. remark (ii)], the sequence of the classical model suggests a growth rate  $\lambda \approx 2$ .

(vii) The growth rate of the  $\Delta_n$  sequence is an important piece of information in approximation schemes used for the reconstruction of spectral densities from a finite number of recurrences. Practically all approximation schemes proposed in the past are based on the assumption that  $\lambda = 0$  or 1, even for situations where this is manifestly not the case. A general procedure that takes the necessary generalizations into account is given in Ref. 14.

(viii) Note that the growth rate  $\lambda = 2$  represents the limiting case of infinite growth order ( $\rho = \infty$ ).  $\Delta_n$  sequences with growth rates  $\lambda \geq 2$  do not represent autocorrelation functions which are entire functions of  $t$ . One case in point is the function (5.13), an exact realization of  $\lambda = 2$ ; its Fourier transform is evidently not entire.

(ix) The number of recurrences that we have been able to compute so far for various cases of the 1D classical  $XYZ$  model is somewhat too small to detect or rule out deviations from the borderline growth rate  $\lambda = 2$  with some confidence. The  $\Delta_n$  sequence of  $\langle S_i^x(t)S_i^x \rangle$  for the  $XX$  model suggests  $\lambda > 2$  (see Fig. 5), while the corresponding sequence for the Heisenberg model ( $XXX$  case) indicates  $\lambda < 2$ . Further work with more computational power is needed.

(x) Time-dependent correlation functions with singularities are not unheard of in otherwise well-behaved classical many-body systems with Hamiltonian dynamics. For the case of the completely integrable logarithmic Heisenberg model<sup>25</sup>

$$H = - \sum_{i=1}^N \ln(1 + \mathbf{S}_i \cdot \mathbf{S}_{i+1}), \quad (6.2)$$

such singularities even make it to the real  $t$  axis, at least for finite  $N$ . The exact result for the  $T = \infty$  autocorrela-

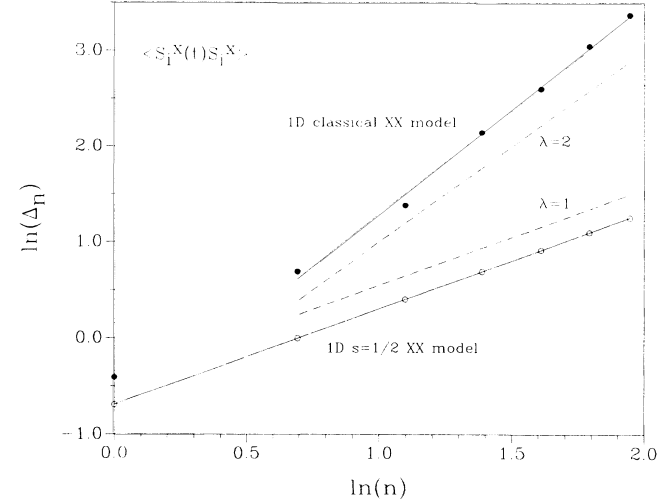


FIG. 5. Log-log plot of sequences  $\Delta_n$  vs  $n$ ,  $n = 1, \dots, 7$ , for the autocorrelation function  $\langle S_i^x(t)S_i^x \rangle$  at  $T = \infty$  of the 1D classical and quantum spin- $\frac{1}{2}$   $XX$  model. The sequence for the quantum model is exactly known,  $\Delta_n = n/2$ , for arbitrary  $n$ . The (solid) regression line determined for  $\Delta_2, \dots, \Delta_7$  of the classical model has slope  $\lambda \approx 2.19$ . Lines with slope  $\lambda = 1$  and 2 are shown by the dashed line.

tion function for  $N = 2$  reads

$$\begin{aligned} A_0(t) = & \frac{1}{2} + \frac{1}{2}(1 + \frac{1}{6}t^2)\cos t - t(\frac{5}{6} + \frac{1}{12}t^2)\sin t \\ & + t^2(1 + \frac{1}{12}t^2)\text{ci}(t) \\ = & t^2(1 + \frac{1}{12}t^2)\ln t + r(t), \end{aligned} \quad (6.3)$$

where  $r(t)$  is regular. Such functions are no longer describable in terms of  $\Delta_n$  sequences.

(xi) In the context of the equivalent-neighbor  $XYZ$  model we have found that the growth rate of  $\Delta_n$  sequences is determined in part by the detailed spectral properties of individual nonlinear modes. It is therefore conceivable that the manifestly different spectral properties of chaotic phase-space trajectories in nonintegrable models have some observable and analyzable impact on the growth rate of  $\Delta_n$  sequences.

## ACKNOWLEDGMENTS

We thank G. R. Verma, M. P. Nightingale, M. H. Lee, J. H. H. Perk, and M. E. Fisher for valuable comments and suggestions. This work was supported by the U.S. National Science Foundation, Grant No. DMR-90-07540. Access to supercomputers at the National Center for Supercomputing Applications, University of Illinois at Urbana-Champaign and at the NASA-Ames Research Center is gratefully acknowledged.

- <sup>1</sup>H. E. Stanley, *Introduction to Phase Transitions and Critical Phenomena* (Oxford University Press, New York, 1971).
- <sup>2</sup>C. Kittel and H. Shore, *Phys. Rev.* **138**, A1165 (1965); T. Niemeijer, *Physica* **48**, 467 (1970); G. Vertogen and A. S. de Vries, *ibid.* **59**, 634 (1972); H. Falk, *Phys. Rev. B* **5**, 3638 (1972); R. Botet and R. Jullien, *ibid.* **28**, 3955 (1983); G. F. Kvetsel and J. Katriel, *ibid.* **30**, 2828 (1984).
- <sup>3</sup>S. K. Ma, *Modern Theory of Critical Phenomena* (Benjamin/Cummings, Reading, MA, 1976).
- <sup>4</sup>M. E. Fisher, *Rev. Mod. Phys.* **46**, 597 (1974).
- <sup>5</sup>The term "intrinsic dynamics" as used here refers to the classical or quantum Hamiltonian dynamics of the microscopic degrees of freedom, excluding any amount of contraction in the level of description.
- <sup>6</sup>This does not exclude meaningful and potentially interesting dynamical studies of equivalent-neighbor spin models at finite temperature by use of effective dynamics.
- <sup>7</sup>If all  $J_\alpha$  have the same sign, the orbits of  $\sigma$  are equivalent to those of the angular momentum vector in the body frame of a free asymmetric top with principal moments of inertia  $I_\alpha = 1/|J_\alpha|$ . Equations (2.4) are then equivalent to Euler's equations. For initial conditions which lead to  $k^2 > 1$ , use the relations  $cn(x, k) = dn(kx, k^{-1})$ ,  $sn(x, k) = k^{-1}sn(kx, k^{-1})$ , and  $dn(x, k) = cn(kx, k^{-1})$ .
- <sup>8</sup>L. van Hemmen, *Fortschr. Phys.* **26**, 397 (1978), previously arrived at Euler's equations for the motion of the collective spin in the quantum equivalent-neighbor XYZ model by an analysis based on  $C^*$  algebra.
- <sup>9</sup>E. Magyari, H. Thomas, R. Weber, C. Kaufman, and G. Müller, *Z. Phys. B* **65**, 363 (1987).
- <sup>10</sup>N. Srivastava, C. Kaufman, G. Müller, R. Weber, and H. Thomas, *Z. Phys. B* **70**, 251 (1988).
- <sup>11</sup>J.-M. Liu and G. Müller, *J. Appl. Phys.* **67**, 5489 (1990).
- <sup>12</sup>*The Recursion Method and its Applications*, edited by D. G. Pettifor and D. L. Weaire (Springer-Verlag, New York, 1985).
- <sup>13</sup>M. H. Lee, *Phys. Rev. B* **26**, 2547 (1982); *Phys. Rev. Lett.* **49**, 1072 (1982); *J. Math. Phys.* **24**, 2512 (1983).
- <sup>14</sup>V. S. Viswanath and G. Müller, *J. Appl. Phys.* **67**, 5486 (1990).
- <sup>15</sup>R. Dekeyser and M. H. Lee, *Phys. Rev. B* **19**, 265 (1979); M. H. Lee, I. M. Kim, and R. Dekeyser, *Phys. Rev. Lett.* **52**, 1579 (1984); R. Dekeyser and M. H. Lee (unpublished).
- <sup>16</sup>See also G. F. Kvetsel and J. Katriel, *Phys. Rev. B* **31**, 1559 (1985).
- <sup>17</sup>The essentially classical character of the quantum equivalent-neighbor spin dynamics is also evident in the analysis performed in Ref. 8.
- <sup>18</sup>A. Magnus, Ref. 12, p. 22; D. S. Lubinsky, *Acta Applicandae Math.* **10**, 237 (1987).
- <sup>19</sup>G. Müller, *J. Phys. (Paris)* **C8**, 1403 (1988).
- <sup>20</sup>N. Srivastava, C. Kaufman, and G. Müller, *J. Appl. Phys.* **63**, 4154 (1988).
- <sup>21</sup>In such models, intrinsic dynamics and the study of growth rates are not, of course, limited to  $T = \infty$ .
- <sup>22</sup>J. M. R. Roldan, B. M. McCoy, and J. H. H. Perk, *Physica A* **136**, 255 (1986).
- <sup>23</sup>J. Florencio and M. H. Lee, *Phys. Rev. B* **35**, 1835 (1987).
- <sup>24</sup>H. Araki, *Commun. Math. Phys.* **14**, 120 (1969).
- <sup>25</sup>Y. Ishimori, *J. Phys. Soc. Jpn.* **51**, 3417 (1982); F. D. M. Haldane, *J. Phys. C* **15**, L1309 (1982); N. Papanicolaou, *J. Phys. A* **20**, 2637 (1987).